

# Design of Rate-Compatible Anytime Codes Based on Spatially Coupled Repeat-Accumulate Codes

Xiaoxi Yu<sup>1</sup>, Md. Noor-A-Rahim<sup>2</sup>, Yong Liang Guan<sup>3</sup>, *Senior Member, IEEE*,  
Li Deng<sup>4</sup>, Zhaojie Yang<sup>5</sup>, and Zhiping Shi<sup>6</sup>

**Abstract**—Anytime code is a new class of error-correcting code that has very long coding memory and is decodable with flexible decoding window size (decoding delay). It is designed for real-time reliable applications, such as tracking and controlling unstable systems. In this paper, we construct a family of rate-compatible (RC) Anytime code ensembles with code rate from 0 to 1 based on spatially coupled repeat-accumulate (SC-RA) codes and apply them to the automatic-repeat-request (ARQ) communication with incremental redundancy. Using density evolution (DE) analysis, we prove that each element code within the RC family has superior Anytime-reliable properties over the binary erasure channel (BEC) and the binary-input additive white Gaussian noise (BI-AWGN) channel. In addition, we develop an expanding-window IR-HARQ (incremental redundancy hybrid automatic-repeat-request) scheme for the proposed RC Anytime codes. Simulation results testify that our proposed RC Anytime codes have better decoding performance than the prior-art RC Anytime codes. Furthermore, when combined with the proposed expanding-window IR-HARQ scheme, our proposed RC Anytime codes show significant advantages over the conventional RC low-density parity-check (LDPC) codes and RC polar codes in the conventional CRC-based IR-HARQ communication systems.

**Index Terms**—Anytime codes, spatially coupled codes, rate-compatible codes, BEC, AWGN channel, IR-HARQ.

Manuscript received 15 September 2022; revised 21 February 2023, 27 May 2023, and 1 August 2023; accepted 5 September 2023. Date of publication 14 September 2023; date of current version 17 January 2024. This work was supported by A\*STAR under its RIE2020 Advanced Manufacturing and Engineering (AME) Industry Alignment Fund - Pre Positioning (IAF-PP) under Grant No. A19D6a0053, in part by the National Research Foundation, Singapore and Infocomm Media Development Authority under its Future Communications Research & Development Programme under Grant No. FCP-NTU-RG-2022-020, in part by the National Natural Science Foundation of China under Grant 62371101. The associate editor coordinating the review of this article and approving it for publication was J. Ha. (*Corresponding author: Yong Liang Guan.*)

Xiaoxi Yu, Yong Liang Guan, and Zhaojie Yang are with the School of Electrical and Electronic Engineering, Nanyang Technological University, Singapore 639798 (e-mail: xiaoxi001@e.ntu.edu.sg; eylguan@ntu.edu.sg; zhaojie.yang@ntu.edu.sg).

Md. Noor-A-Rahim is with the School of Computer Science and IT, University College Cork, Cork, T12 K8AF Ireland (e-mail: m.rahim@cs.ucc.ie).

Li Deng is with the National Key Laboratory on Communications, University of Electronic Science and Technology of China, Chengdu 610056, China, and also with the School of Electronic Information and Automation, Guilin University of Aerospace Technology, Guilin 541004, China (e-mail: dengli@std.uestc.edu.cn).

Zhiping Shi is with the National Key Laboratory on Communications, University of Electronic Science and Technology of China, Chengdu 610056, China (e-mail: szp@uestc.edu.cn).

Color versions of one or more figures in this article are available at <https://doi.org/10.1109/TCOMM.2023.3315314>.

Digital Object Identifier 10.1109/TCOMM.2023.3315314

0090-6778 © 2023 IEEE. Personal use is permitted, but republication/redistribution requires IEEE permission.  
See <https://www.ieee.org/publications/rights/index.html> for more information.

## I. INTRODUCTION

ANYTIME information theory was introduced by Anant Sahai and has been proven to play a significant role in tracking unstable processes and controlling unstable plants over a noisy channel [1]. Different from the classical coding theory, which aims to achieve error-free decoding performance with infinite decoding delays (i.e., infinite decoding window size), the Anytime information theory requires the code's decoding error probabilities to decay exponentially with the decoding delays [2]. In other words, the code's decoding success rate improves with the growth of the decoding window size. In Anytime-coded transmission, a new performance metric, named *delay-exponent*, is defined to describe the decaying speed of the asymptotic decoding error probability with decoding delay. Codes that possess positive delay-exponent are said to have *Anytime-reliable properties* and can be named as *Anytime codes* [3].

In [4] and [5], the authors proven that linear Anytime-reliable codes exist with high probability. Later, it was found in [6] that random linear tree codes have the Anytime-reliable properties. These discoveries inspired researchers to turn their attention to the design of practical Anytime codes over various channels and systems. In [3], [7], [8], and [9], the authors proposed a protograph-based low-density parity-check (LDPC) convolutional code and proved its Anytime-reliable properties by deriving the delay-exponent over the binary erasure channels (BEC) and the binary-input additive white Gaussian noise (BI-AWGN) channel, respectively. Another class of Anytime codes based on the spatially coupled LDPC (SC-LDPC) codes [10] was also shown to have the Anytime-reliable properties over the BEC. Recent papers [11], [12] dedicate to improving the decoding error performance of the aforementioned Anytime codes. Furthermore, a new class of joint source channel Anytime coding (JSCAC) scheme was designed in [13]. Applications of the Anytime codes in the relay channel transmissions can be found in [14], and the investigation of the Anytime-coded communications in chaotic systems was shown in [15].

A typical scenario in which the Anytime codes are used is wireless automation, where a remote controller requires the real-time state information of a plant to determine the next action. One problem with wireless communication systems is that the channels are time-varying. Therefore, in order

to maximize the throughput, it is essential to design rate-compatible (RC) Anytime codes that can adapt to varying channel conditions with the use of incremental redundancy hybrid automatic-repeat-request (IR-HARQ) scheme [16]. This class of RC family, constructed through graph extension,<sup>1</sup> consists of a set of codes with different code rates, where a high-rate code, referred to as the *mother code*, is progressively extended to codes of lower rates. In IR-HARQ, the high-rate mother code is sent first, and the incremental redundancy (IR) parity bits in the lower-rate codes will be sent later if requested from the receiver when error correction fails. Then the receiver combines all received coded bits, old and new, to recover the information.

A type of RC Anytime codes has already been designed in [9]. However, these codes have limited code rates and suffer from high encoding and decoding complexity. This inspired us to design new RC Anytime codes that have simpler code structure, a wider range of code rates, and better Anytime-reliable properties.

In this paper, we propose an RC Anytime code ensemble based on regular spatially coupled repeat-accumulate (SC-RA) codes. The novel contributions are summarized as follows:

- 1) We thoroughly analyze the Anytime  $(Q, A, \lambda)$ -ensemble. Specifically, we derive the general delay-exponent formulas (i.e., prove the Anytime-reliable properties) of the code ensemble over the BEC and the BI-AWGN channel, respectively, for the first time. Using the delay-exponent, we compare the Anytime SC-RA codes with the prior-art Anytime codes and show that the Anytime  $(Q, A, \lambda)$ -ensemble outperforms others in terms of Anytime-reliable properties and decoding complexity. This superiority makes the Anytime SC-RA codes a good mother code for constructing the RC Anytime codes.
- 2) We design an RC Anytime  $(Q_1, Q_2, A_1, A_2, \lambda)$ -ensemble by extending the coupled-protograph of Anytime  $(Q, A, \lambda)$ -ensemble. We prove that the RC family constructed from this ensemble can possess arbitrary (rational) design rates ranging from 0 to 1, and allow every code ensemble in the family to have a guaranteed large delay-exponent over both BEC and BI-AWGN channel.
- 3) We design an expanding-window IR-HARQ scheme for the applications of the proposed RC Anytime codes in the automatic-repeat-request (ARQ) communication scenarios.
- 4) By conducting simulations over both BEC and BI-AWGN channels, we demonstrate the effectiveness of our proposed RC Anytime codes and the proposed expanding-window IR-HARQ scheme. Our results show that our proposed codes outperform prior-art RC Anytime codes and conventional RC error-correction codes.

<sup>1</sup>Generally, there are two methods to construct the RC codes: puncturing [17] and graph extension [18], [19]. It was shown in [19] that the graph extension method outperforms the puncturing method by resulting in RC codes that have smaller gaps to capacity. Hence we only consider the graph extension method in this paper.

The paper is structured as follows. In Section II, we introduce Anytime-coded transmission. In Section III, we first show a good mother code ensemble with in-depth analysis, then use it to construct an RC Anytime SC-RA code ensemble and the corresponding RC family. In addition, we design an IR-HARQ scheme based on the proposed RC Anytime codes. The simulation results are shown in Section IV, followed by concluding summaries in Section V.

## II. ANYTIME-CODED TRANSMISSION

Considering a source produces a  $K$ -bit information block  $\mathbf{m}_i \in \{0, 1\}^K$  at every time index  $i$ . When  $i = t$ , the source has produced an information stream  $\mathbf{m}_{[1,t]} = [\mathbf{m}_1, \mathbf{m}_2, \dots, \mathbf{m}_t]$ .

At time instant  $t$ , the Anytime channel encoder encodes all the information stream  $\mathbf{m}_{[1,t]}$  received so far into a fixed-length  $N$ -bit block  $\mathbf{x}_t \in \{0, 1\}^N$  using an encoding function  $\mathbf{x}_t = \varepsilon_t(\mathbf{m}_{[1,t]})$ . The code block  $\mathbf{x}_t$  is transmitted over a noisy binary memoryless channel, and received as  $\bar{\mathbf{x}}_t$  (a corrupted version of  $\mathbf{x}_t$ ) by the Anytime channel decoder. Based on all received blocks  $\bar{\mathbf{x}}_{[1,t]} = [\bar{\mathbf{x}}_1, \bar{\mathbf{x}}_2, \dots, \bar{\mathbf{x}}_t]$ , the decoder produces estimates  $\hat{\mathbf{x}}_{[1,t]} = [\hat{\mathbf{x}}_1, \hat{\mathbf{x}}_2, \dots, \hat{\mathbf{x}}_t]$  by the decoding function  $\hat{\mathbf{x}}_{[1,t]} = D_t(\bar{\mathbf{x}}_{[1,t]})$ . Finally,  $\hat{\mathbf{x}}_{[1,t]}$  are used to produce an estimated streaming source  $\hat{\mathbf{m}}_{[1,t]}$ . In this way, the decoder can decide to start decoding at any time and can provide an estimate of any information block  $\mathbf{m}_i$  transmitted so far at any time, which is the reason for the terminology *Anytime*.

*Definition 1 (Anytime reliability):* As proven in [1], the *Anytime reliability* of the system is defined as

$$P_e(i, t) = P_e(i, i + d) \leq \beta e^{-\alpha d}, \quad \forall d \geq 0, \quad (1)$$

where  $P_e(i, t) = P_r(\hat{\mathbf{m}}_i(t) \neq \mathbf{m}_i \mid \mathbf{x}_{[1,t]}$  was transmitted) is the probability of error of the  $i$ -th decoded information  $\hat{\mathbf{m}}_i$  at time instant  $t$ ,  $d = t - i$  is the decoding delay,  $\beta$  is a positive constant whose value is decided by the channel properties, and  $\alpha > 0$  is known as the *delay-exponent*.

In this definition, for any fixed  $i \in \mathbb{N}$ , the error probability will decrease exponentially with the decoding delay  $d$ , for  $d \geq 0$ , to an arbitrarily small value. The delay-exponent  $\alpha$  measures the decaying speed of  $P_e(i, i + d)$  as the decoding delay  $d$  grows unbounded, i.e.,  $-\alpha$  is the slope of the  $P_e(i, i + d)$  curve, and it is the most important performance metric of Anytime-coded transmission.

*Definition 2 (Anytime-reliable property):* An error correction code, together with the encoder-decoder pair  $(\varepsilon_t, D_t)$ , is said to have *Anytime-reliable properties* and can be named as *Anytime code* if it can achieve the *Anytime reliability* when used in Anytime-coded transmission.

In other words, a code that exhibits the Anytime-reliable property has an asymptotic decoding error probability  $P_e(i, i + d)$  that satisfies (1) with a positive *delay-exponent*  $\alpha$  for all  $i, d \in \mathbb{N}$ , where  $\alpha$  is defined as [11]

$$\alpha \triangleq \lim_{d \rightarrow \infty} \left( \lim_{i \rightarrow \infty} -\frac{\log P_e(i, i + d)}{d} \right). \quad (2)$$

## III. PROPOSED: RATE-COMPATIBLE (RC) ANYTIME SC-RA CODES

In this section, we will first introduce a good mother code ensemble (the Anytime SC-RA code ensemble) by proving

its Anytime-reliable properties in Section III-A. After that, we will show how we construct the RC Anytime SC-RA code ensemble and form a corresponding family in Sections III-B and III-C, respectively. We will prove analytically that the proposed RC Anytime codes have outstanding Anytime-reliable properties over both BEC and BI-AWGN channel. Later, in Section III-D, we will put forward an expanding-window IR-HARQ scheme for the proposed RC Anytime codes.

Note that while we use protograph-based SC-RA codes to construct Anytime codes, the asymptotic analysis (including the code rate and density evolution) relies on random-structured SC-RA codes (see the difference in Section II of [24]), which simplifies the derivation of equations. Nevertheless, thanks to the simple protograph structure of SC-RA codes, the accuracy of these analysis results can still be guaranteed for the proposed Anytime SC-RA codes.

#### A. Mother Code Ensemble: Anytime $(Q, A, \lambda)$ -Ensemble

Anytime SC-RA codes can be formed by spatially coupling a series of uncoupled  $(Q, A)$ -regular repeat-accumulate (RA) codes. Fig. 1(a) shows the protograph of a standard  $(Q, A)$ -regular RA code: there is an *information bit node* (IN) on the top, a *parity check node* (CN) in the middle, and a *parity bit node* (PN) at the bottom. The IN and CN degrees are  $Q$  and  $A$ , respectively. The PN has a fixed two-edge connection to the CN.

The construction of the Anytime SC-RA code ensemble, also referred to as the Anytime  $(Q, A, \lambda)$ -ensemble, follows a similar approach to that used for the Anytime SC-LDPC code ensemble [10]:

- 1) The chain length  $L$  and the coupling width  $w$  are considered to be very large so that the bits at every position can have independent reliability performance.
- 2) To generate the coupled protograph, each IN at position  $i \in L$  is connected to the CNs at positions  $j \in \{i, \dots, i + w - 1\}$  following an exponential distribution,<sup>2</sup> i.e., the probability of an edge connected between positions  $i$  and  $j$  is

$$P_r(k) = \frac{e^{-k\lambda}(1 - e^{-\lambda})}{1 - e^{-w\lambda}}, \quad (3)$$

where  $k = j - i$  is the position difference between  $i$  and  $j$ , and  $\lambda$  is the exponential coupling rate representing the degree of concentration of the distribution. For  $w \rightarrow \infty$ , (3) becomes

$$P_r(k) = e^{-k\lambda}(1 - e^{-\lambda}). \quad (4)$$

In Fig. 1(b), we show the protograph chain structure of the Anytime  $(Q, A, \lambda)$ -ensemble. Within the chain, each protograph position represents one time constant, hence the chain length  $L$  will increase in  $t$  with one protograph position at a time. The code rate is given as

$$R(Q, A, \lambda) = \frac{A}{A + Q \frac{[L+w+1+\sum_{i=0}^{w-1}(1-\sum_{k=0}^i P_r(k))^A]}{L}}. \quad (5)$$

<sup>2</sup>Since we are having a large coupling length, using exponential distribution allows a quick improvement of the error performance with a small delay while maintaining the low-density structure of the parity-check matrix.

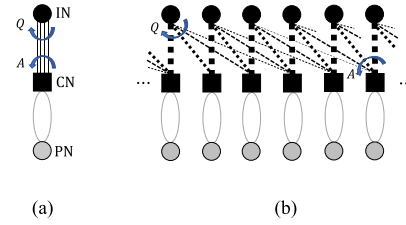


Fig. 1. (a) A RA protograph with  $Q = 4$  and  $A = 4$ . (b) Protographs of the Anytime  $(Q, A, \lambda)$ -ensemble. The edges connected between INs and CNs are drawn in dotted lines to represent the exponentially distributed connection probabilities: the thicker the line is, the higher the probability that this connection will happen.

Therefore, for  $w \rightarrow \infty$  and  $L \rightarrow \infty$ , the design rate is  $\lim_{w \rightarrow \infty, L \rightarrow \infty} R(Q, A, \lambda) = \frac{A}{A+Q}$ .

The convolutional base matrix corresponding to the Anytime  $(Q, A, \lambda)$ -ensemble up to time  $t$  is

$$\mathbf{B}_{[0,t-1]} = \begin{bmatrix} \mathbf{B}_0 & & & & \\ \mathbf{B}_1 & \mathbf{B}_0 & & & \\ \vdots & \vdots & \ddots & & \\ \mathbf{B}_{t-1} & \mathbf{B}_{t-2} & \cdots & \mathbf{B}_0 & \end{bmatrix}. \quad (6)$$

In (6), the *component base matrices*  $\mathbf{B}_k$ ,  $0 \leq k \leq t - 1$ , can be further written as  $\mathbf{B}_0 = [\mathbf{Z}_0 \mathbf{Z}_{\text{RA}}]$  for  $k = 0$  and  $\mathbf{B}_k = [\mathbf{Z}_k \mathbf{0}]$  for  $1 \leq k \leq t - 1$ . Here, the  $b_c \times b_v$  *sub-component base matrices*  $\mathbf{Z}_k$  represents the edge connections from the  $b_v$  INs at position  $i$  to the  $b_c$  CNs which are  $k$  positions away from it (i.e., the upper part connections in Fig. 1(b)), where  $b_c = \frac{Q}{A} b_v$ .  $\mathbf{Z}_{\text{RA}}$  is a  $b_c \times b_c$  matrix due to the accumulator [20] (i.e., the lower part connections in Fig. 1(b)). By performing the lifting operation [21] on the coupled-protograph (the convolutional base matrix  $\mathbf{B}_{[0,t-1]}$ ) with a lifting factor  $M$ , the Tanner graph (the parity-check matrix  $\mathbf{H}_{[0,t-1]}$ ) of the Anytime SC-RA codes can be constructed, where each position now contains  $n_v = b_v M$  INs,  $n_c = b_c M$  CNs and  $n_c$  PNs. In the Anytime-coded transmission, such codes can be encoded using the syndrome former encoder [22] and decoded by the expanding-window message passing decoder [8] thanks to the lower-triangular structure of the parity-check matrix.

In the following parts, we use density evolution (DE) analysis [23] to evaluate the Anytime-reliable properties of the  $(Q, A, \lambda)$ -ensemble (i.e., deriving the delay-exponent) for the first time. It's worth noting that our derivation method is more concise than the approaches adopted in [3], [10], and [11].

1) *BEC*: First, we consider the DE analysis over BEC. DE algorithm analyzes the asymptotic performance of the codes under the assumption that the block length tends to infinity. In the  $l$ -th iteration at time  $t$ , we define  $p^l(i, t)$  and  $p_p^l(j, t)$  as the erasure probability of the message from an IN at position  $i$  and a PN at position  $j$ , respectively; we also define  $q^l(j, t)$  and  $q_p^l(j, t)$  as the erasure probability of the message from a CN at position  $j$  to an IN and a PN, respectively. Similar to [10], the DE equations of the Anytime  $(Q, A, \lambda)$ -ensemble over a BEC with channel erasure

probability  $\epsilon$  are

$$\begin{aligned}
q^l(j, t) &= 1 - \left(1 - \sum_{k=0}^{\infty} P_r(k) p^l(j-k, t)\right)^{A-1} \\
&\quad \cdot (1 - p_p^l(j, t))^2, \\
p^{l+1}(i, t) &= \epsilon \left(\sum_{j=0}^{t-i} P_r(j) q^l(i+j, t)\right)^{Q-1}, \\
q_p^l(j, t) &= 1 - \left(1 - \sum_{k=0}^{\infty} P_r(k) p^l(j-k, t)\right)^A \cdot (1 - p_p^l(j, t)), \\
p_p^{l+1}(j, t) &= \epsilon \cdot q_p^l(j, t).
\end{aligned}$$

Therefore, the erasure probability of IN at position  $i$  after an infinite number of iterations is

$$\begin{aligned}
P_e^{\text{BEC}}(i, t) &= \epsilon \left\{ 1 - \sum_{j=0}^{t-i} P_r(j) \right. \\
&\quad \cdot \left[ \left(1 - \sum_{k=0}^{\infty} P_r(k) p^\infty(i+j-k, t)\right)^{A-1} \right. \\
&\quad \left. \left. \cdot (1 - p_p^\infty(i+j, t))^2 \right] \right\}^Q. \quad (7)
\end{aligned}$$

*Lemma 1:* Given a BEC erasure probability  $\epsilon$  such that  $\epsilon \leq \epsilon^{\text{MAP}}(Q, A)$ , where  $\epsilon^{\text{MAP}}(Q, A)$  is the maximum a posteriori (MAP) threshold of the underlying RA protograph  $(Q, A)$ -ensemble, the delay-exponent  $\alpha_{\text{BEC}}$  of the Anytime  $(Q, A, \lambda)$ -ensemble is given as

$$\alpha_{\text{BEC}}(Q, A, \lambda) = \lambda Q.$$

*Proof:* We provide the fact that, in the DE analysis of the protograph-based SC-RA codes over a BEC with channel erasure probability  $\epsilon$ , the erasure probability of the message from an IN (or from a PN) will approach zero after an infinite number of iterations for  $\epsilon \leq \epsilon^{\text{MAP}}(Q, A)$ , where  $\epsilon^{\text{MAP}}(Q, A)$  is the MAP threshold of the underlying RA protograph  $(Q, A)$ -ensemble, i.e., the *threshold saturation* phenomenon (see evidence in Appendix A). Therefore, for  $\epsilon \leq \epsilon^{\text{MAP}}(Q, A)$ , the Anytime  $(Q, A, \lambda)$ -ensemble have  $p^\infty(i, t) = 0$  and  $p_p^\infty(i, t) = 0$  for (7)

$$\begin{aligned}
\lim_{t \rightarrow \infty} P_e^{\text{BEC}}(i, t) &= \epsilon \left\{ 1 - \sum_{j=0}^d P_r(j) \right. \\
&\quad \cdot \left[ \left(1 - \sum_{k=0}^{\infty} P_r(k) \cdot 0\right)^{A-1} (1-0)^2 \right] \right\}^Q \\
&= \epsilon \left\{ 1 - \sum_{j=0}^d P_r(j) \cdot 1 \right\}^Q \\
&\stackrel{(a)}{=} \epsilon \left\{ 1 - (1 - e^{-\lambda}) \sum_{j=0}^d e^{-j\lambda} \right\}^Q \\
&= \epsilon \left\{ 1 - (1 - e^{-\lambda}) \frac{1 - e^{-\lambda(d+1)}}{1 - e^{-\lambda}} \right\}^Q \\
&= \epsilon \cdot e^{-\lambda Q(d+1)}, \quad (8)
\end{aligned}$$

TABLE I

DELAY-EXPONENT  $\alpha_{\text{BEC}}$  OVER BEC ( $\epsilon = 0.3$ ), AVERAGE VARIABLE NODE DEGREE  $\bar{d}_v$  AND AVERAGE CHECK NODE DEGREE  $\bar{d}_c$  FOR DIFFERENT ANYTIME CODE ENSEMBLES WITH DESIGN RATE  $R = 0.5$

	$\alpha_{\text{BEC}}$	$\bar{d}_v$	$\bar{d}_c$
Anytime RA (4, 4, 0.5)	2	3	6
Anytime RA (6, 6, 0.5)	3	4	8
Anytime LDPC (3, 6, 0.5) [10]	1.5	3	6
Anytime LDPC (5, 10, 0.5) [10]	2.5	5	10
Anytime Convolutional LDPC [8]	1.737	$\infty$	$\infty$

where in (a) we use (4) for  $P_r(j)$ . Thus, by replacing (8) into (2), we obtain

$$\begin{aligned}
\alpha_{\text{BEC}}(Q, A, \lambda) &= \lim_{d \rightarrow \infty} \left( \lim_{i \rightarrow \infty} - \left( \frac{\log \epsilon}{d} + \frac{-\lambda Q(d+1)}{d} \right) \right) \\
&= \lim_{d \rightarrow \infty} \left( \lim_{i \rightarrow \infty} - \left( -\lambda Q \left(1 + \frac{1}{d}\right) + \frac{\log \epsilon}{d} \right) \right) \\
&= \lambda Q - \lim_{d \rightarrow \infty} \left( \lim_{i \rightarrow \infty} \left( \frac{-\lambda Q}{d} + \frac{\log \epsilon}{d} \right) \right) \\
&= \lambda Q.
\end{aligned}$$

In Table I, we compare  $\alpha_{\text{BEC}}$  of the proposed Anytime  $(Q, A, \lambda)$ -ensemble with the Anytime SC-LDPC code ensemble [10] and the Anytime convolutional LDPC code ensemble [8]. Notice that, while the average node degrees are fixed for the two exponential-structured ensembles, the convolutional LDPC ensemble [8] is designed to have its  $\bar{d}_v$  and  $\bar{d}_c$  increase quadratically with the decoding delay, hence the entries are set as infinities. It can be observed that the proposed  $(Q, A, \lambda)$ -ensemble exhibits the largest  $\alpha_{\text{BEC}}$  with the lowest decoding complexity (as measured by the Tanner graph edge density) compared with the other two prior-art Anytime codes. For example, the Anytime RA (4, 4, 0.5)-ensemble has  $\alpha_{\text{BEC}} = 2$  which is 0.5 higher than that of the Anytime LDPC (3, 6, 0.5)-ensemble with the same average nodes degrees. Moreover, when compared with the Anytime convolutional LDPC ensemble that suffers from high decoding complexity, the Anytime RA (4, 4, 0.5)-ensemble still shows a 0.236 gain in  $\alpha_{\text{BEC}}$ .

2) *BI-AWGN Channel:* In the  $l$ -th iteration at time  $t$ , we define  $x^l(i, t)$  and  $x_p^l(j, t)$  to be the probability density function (pdf) for a message sent from an IN at position  $i$  and a PN at position  $j$ , respectively;  $y^l(j, t)$  and  $y_p^l(j, t)$  to be the pdf for a message sent from a CN at position  $j$  to an IN and a PN, respectively. We further define  $a$  to be the pdf for the transmitted BI-AWGN channel. Note that all the messages considered here are the log-likelihood ratios (LLRs) [20] and the operator  $\otimes$  denotes the convolution process.

The DE equations of the Anytime  $(Q, A, \lambda)$ -ensemble over the BI-AWGN channel are

$$\begin{aligned}
y^l(j, t) &= \left( \sum_{k=0}^{\infty} P_r(k) x^l(j-k, t) \right)^{\otimes(A-1)} \otimes x_p^l(j, t)^{\otimes 2}, \\
x^{l+1}(i, t) &= a \otimes \left( \sum_{j=0}^{t-i} P_r(j) y^l(i+j, t) \right)^{\otimes(Q-1)},
\end{aligned}$$

$$y_p^l(j, t) = \left( \sum_{k=0}^{\infty} P_r(k) x^l(j-k, t) \right)^{\otimes A} \otimes x_p^l(j, t),$$

$$x_p^{l+1}(j, t) = a \otimes y_p^l(j, t).$$

Thus, we can derive the pdf of the error probability of IN at position  $i$

$$P_e^{\text{AWGN}}(i, t) = a \otimes \left\{ \sum_{j=0}^{t-i} P_r(j) \otimes \left[ \left( \sum_{k=0}^{\infty} P_r(k) x^{\infty}(i+j-k, t) \right)^{\otimes (A-1)} \otimes x_p^{\infty}(i+j, t)^{\otimes 2} \right] \right\}^{\otimes Q}. \quad (9)$$

*Lemma 2:* Given a BI-AWGN channel noise variance  $\sigma_n^2$  such that  $\sigma_n \leq \sigma_n^{\text{MAP}}(Q, A)$ , where  $\sigma_n^{\text{MAP}}(Q, A)$  is the MAP threshold of the underlying RA protograph  $(Q, A)$ -ensemble over BI-AWGN channel, the lower bound of the delay-exponent of the Anytime  $(Q, A, \lambda)$ -ensemble is given as

$$\underline{\alpha}_{\text{AWGN}}(Q, A, \lambda) = 0.175\lambda Q.$$

The proof of the lemma is long, hence we relegate it to Appendix B. Table II<sup>3</sup> provides the comparison on  $\underline{\alpha}_{\text{AWGN}}$  of the proposed Anytime  $(Q, A, \lambda)$ -ensemble and the Anytime convolutional LDPC ensemble [8] whose  $\underline{\alpha}_{\text{AWGN}}$  was proven in [7]. It can be observed that the Anytime  $(Q, A, \lambda)$ -ensemble always achieves a higher  $\underline{\alpha}_{\text{AWGN}}$  than the Anytime convolutional LDPC ensemble while maintaining a low graph edge density.

Based on the analysis above, we remark that the  $(Q, A, \lambda)$ -ensemble can achieve superior Anytime-reliable properties over both BEC and BI-AWGN channel with low decoding complexity compared with the prior-art Anytime codes, hence we will use it as the mother code to construct the new RC Anytime codes. It is worth noting that, although the delay-exponent  $\alpha$  evaluates the asymptotic achievable decaying speed of the bit-erasure rate (or bit-error rate) with respect to the decoding delay, in actual implementation, the Anytime codes possessing larger  $\alpha$  were also observed to have a faster decay of the bit-erasure rate (or bit-error rate) curve.

### B. RC Anytime $(Q_1, Q_2, A_1, A_2, \lambda)$ -Ensemble

To construct an RC Anytime code ensemble from the Anytime  $(Q, A, \lambda)$ -ensemble, we employ the graph extension method [18], [19] and introduce a two-type-connection protograph. As the example shown in Fig. 2(a), we define the CNs and the PNs of the original protograph (drawn in black and grey) as Type-1 nodes, and these nodes are denoted by  $\text{CN}_1$  and  $\text{PN}_1$ , respectively. The edges connection between the INs and the  $\text{CN}_1$  are referred to as Type-1 connection, and the information variable node degree and the check node degree of Type-1 connection are  $Q_1$  and  $A_1$ , respectively. In addition, we define the newly added CNs and PNs (drawn

<sup>3</sup>The SC-LDPC Anytime code ensemble [10] does not have a proven  $\underline{\alpha}_{\text{AWGN}}$  or  $\underline{\alpha}_{\text{AWGN}}$  so it is not included in the comparison.

TABLE II

LOWER BOUND OF THE DELAY-EXPONENT  $\underline{\alpha}_{\text{AWGN}}$  OVER BI-AWGN CHANNELS, AVERAGE VARIABLE NODE DEGREE  $\bar{d}_v$  AND AVERAGE CHECK NODE DEGREE  $\bar{d}_c$  FOR DIFFERENT ANYTIME CODE ENSEMBLES WITH DESIGN RATE  $R = 0.5$

	SNR	$\underline{\alpha}_{\text{AWGN}}$	$\bar{d}_v$	$\bar{d}_c$
Anytime RA (4, 4, 0.5)	0.5dB	0.35	3	6
Anytime Convolutional LDPC [8]		0.25	$\infty$	$\infty$
Anytime RA (10, 10, 0.7)	2dB	1.225	6	12
Anytime Convolutional LDPC [8]		1	$\infty$	$\infty$

in orange) as Type-2 nodes, which are written as  $\text{CN}_2$  and  $\text{PN}_2$ , respectively. The edges connection between the INs and the  $\text{CN}_2$  are referred to as Type-2 connection, where the node degrees of the IN and the  $\text{CN}_2$  are  $Q_2$  and  $A_2$ , respectively.

*Definition 3 (RC Anytime  $(Q_1, Q_2, A_1, A_2, \lambda)$ -Ensemble):* Consider a two-type-connection protograph. In this protograph, each IN has a degree  $Q_1 + Q_2$ , where  $Q_1$  edges connects to  $\text{CN}_1$  and  $Q_2$  edges connects to  $\text{CN}_2$ . Each  $\text{CN}_1$  ( $\text{CN}_2$ ) has  $A_1$  ( $A_2$ ) edges connects to INs and two edges connects to  $\text{PN}_1$  ( $\text{PN}_2$ ). By coupling a number of these two-type-connection protographs and applying the lifting operation, the RC Anytime  $(Q_1, Q_2, A_1, A_2, \lambda)$ -ensemble is constructed, where the  $Q_1$ ,  $Q_2$  and  $A_1$ ,  $A_2$  edges all follow an exponential distribution.

The coupled protograph chain of the RC Anytime  $(Q_1, Q_2, A_1, A_2, \lambda)$ -ensemble is given in Fig. 2(b). This ensemble can be constructed in three steps. First, we add  $b'_c$   $\text{CN}_2$  and  $b'_c$   $\text{PN}_2$  to the protograph of the Anytime  $(Q_1, A_1, \lambda)$ -ensemble, where  $b'_c = \frac{Q_2}{A_2} b_v$ . Therefore, in each protograph, now there are  $b_v$  INs,  $b_c + b'_c$  CNs and  $b_c + b'_c$  PNs in total. In the second step, we couple several of these two-type-connection protographs into a protograph chain. Specifically, the exponential distributed coupling method, introduced in Section III-A, is applied to both the Type-1 and Type-2 connections. The resulting convolutional base matrix up to time  $t$  is

$$\mathbf{B}'_{[0, t-1]} = \begin{bmatrix} \mathbf{B}'_0 & & & \\ \mathbf{B}'_1 & \mathbf{B}'_0 & & \\ \vdots & \vdots & \ddots & \\ \mathbf{B}'_{t-1} & \mathbf{B}'_{t-2} & \cdots & \mathbf{B}'_0 \end{bmatrix}, \quad (10)$$

where

$$\mathbf{B}'_0 = \begin{bmatrix} \mathbf{Z}'_0 & \mathbf{Z}'_{\text{RA}} \end{bmatrix} \quad \text{and} \quad \mathbf{B}'_k = \begin{bmatrix} \mathbf{Z}'_k & \mathbf{0}' \end{bmatrix},$$

for  $1 \leq k \leq t-1$ .  $\mathbf{Z}'_k$  with size  $b_c \times b_v$  and  $\mathbf{Z}'_k$  with size  $b'_c \times b_v$  represents the edge connections from the  $b_v$  INs at position  $i$  to the  $b_c$   $\text{CN}_1$  (Type-1 connection) and the  $b'_c$   $\text{CN}_2$  (Type-2 connection) which are  $k$  positions away from it, respectively.  $\mathbf{Z}'_{\text{RA}}$  is an enlarged RA connection now with a size  $(b_c + b'_c) \times (b_c + b'_c)$ . In the final step, we perform the lifting operation on the convolutional base matrix using a lifting factor  $M$ , thereby constructing the final parity-check matrix  $\mathbf{H}'_{[0, t-1]}$  of the RC Anytime  $(Q_1, Q_2, A_1, A_2, \lambda)$ -ensemble. After the lifting, each position now contain  $n_v = b_v M$  INs,  $n_c + n'_c = (b_c + b'_c) M$  CNs and  $n_c + n'_c = (b_c + b'_c) M$  PNs. The number of the nodes should satisfy  $n_v \cdot Q_1 = n_c \cdot A_1$  and  $n_v \cdot Q_2 = n'_c \cdot A_2$ .

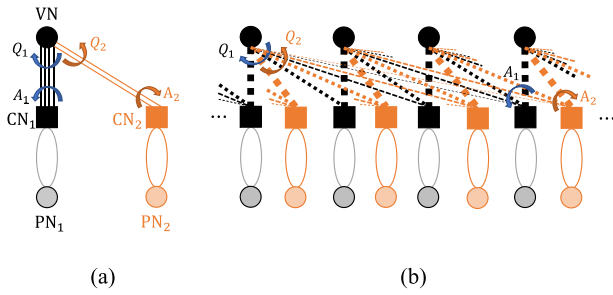


Fig. 2. (a) A two-type-connection RA protograph with  $Q_1 = 4$  and  $Q_2 = 2$ . (b) Protographs of the RC Anytime  $(Q_1, Q_2, A_1, A_2, \lambda)$ -ensemble. The edges connected between INs and two types of CNs are drawn in dotted lines to represent the exponentially distributed connection probabilities.

*Lemma 3: The design rate of the RC Anytime  $(Q_1, Q_2, A_1, A_2, \lambda)$ -ensemble is*

$$\lim_{L \rightarrow \infty} R(Q_1, Q_2, A_1, A_2, \lambda) = \frac{A_1 A_2}{A_1 A_2 + Q_1 A_2 + Q_2 A_1}.$$

*Proof:* Using a similar derivation as in [25], the code rate of a  $(Q_1, Q_2, A_1, A_2, \lambda)$ -ensemble is given by

$$R(Q_1, Q_2, A_1, A_2, \lambda) = \frac{L}{L + L_p}. \quad (11)$$

where

$$L_p = \frac{Q_1}{A_1} \left[ L + w + 1 + \sum_{i=0}^w \left( 1 - \sum_{k=0}^i P_r(k) \right)^{A_1} \right] + \frac{Q_2}{A_2} \left[ L + w + 1 + \sum_{i=0}^w \left( 1 - \sum_{k=0}^i P_r(k) \right)^{A_2} \right].$$

Since the coupling width  $w$  of the proposed codes inherently tends to infinity, as  $L$  tends to infinity, (11) becomes to

$$R(Q_1, Q_2, A_1, A_2, \lambda) = \frac{A_1 A_2}{A_1 A_2 + Q_1 A_2 + Q_2 A_1}.$$

In the sequel, we will analyze the Anytime-reliable properties of the proposed RC Anytime  $(Q_1, Q_2, A_1, A_2, \lambda)$ -ensemble over the BEC and the BI-AWGN channel.

*Theorem 1: In a BEC, the RC Anytime  $(Q_1, Q_2, A_1, A_2, \lambda)$ -ensemble described in Definition 3 can achieve the same delay-exponent as the non-rate-compatible Anytime  $(Q_1 + Q_2, A, \lambda)$ -ensemble if  $A_1 = A_2 = A$ .*

*Proof:* In the  $l$ -th iteration at time  $t$ , we define  $p_1^l(i, t)$  (or  $p_2^l(i, t)$ ),  $p_{p1}^l(j, t)$  and  $p_{p2}^l(j, t)$  as the erasure probability of the message from an IN at position  $i$  along the Type-1 edges (or Type-2 edges), from a  $PN_1$  at position  $j$ , and from a  $PN_2$  at position  $j$ , respectively; we also define  $q_1^l(j, t)$  (or  $q_2^l(j, t)$ ) and  $q_{p1}^l(j, t)$  (or  $q_{p2}^l(j, t)$ ) as the erasure probability of the message from a  $CN_1$  (or  $CN_2$ ) at position  $j$  to an IN and to a  $PN_1$  (or  $PN_2$ ), respectively. Given the channel erasure probability  $\epsilon$ , we initialize  $p_1^0(i, t) = p_{p1}^0(j, t) = p_2^0(i, t) = p_{p2}^0(j, t) = \epsilon$  for  $0 < i, j \leq t$ . The DE equations of the Type-1 connection are

written as

$$q_1^l(j, t) = 1 - \left( 1 - \sum_{k=0}^{\infty} P_r(k) p_1^l(j-k, t) \right)^{A_1-1} \cdot (1 - p_{p1}^l(j, t))^2, \quad (12)$$

$$p_1^{l+1}(i, t) = \epsilon \left( \sum_{j=0}^{t-i} P_r(j) q_1^l(i+j, t) \right)^{Q_1-1} \cdot \left( \sum_{j=0}^{t-i} P_r(j) q_2^l(i+j, t) \right)^{Q_2}, \quad (13)$$

$$q_{p1}^l(j, t) = 1 - \left( 1 - \sum_{k=0}^{\infty} P_r(k) p_1^l(j-k, t) \right)^{A_1} \cdot (1 - p_{p1}^l(j, t)), \quad (14)$$

$$p_{p1}^{l+1}(j, t) = \epsilon \cdot q_{p1}^l(j, t). \quad (15)$$

For the Type-2 connection,

$$q_2^l(j, t) = 1 - \left( 1 - \sum_{k=0}^{\infty} P_r(k) p_2^l(j-k, t) \right)^{A_2-1} \cdot (1 - p_{p2}^l(j, t))^2, \quad (16)$$

$$p_2^{l+1}(i, t) = \epsilon \left( \sum_{j=0}^{t-i} P_r(j) q_1^l(i+j, t) \right)^{Q_1} \cdot \left( \sum_{j=0}^{t-i} P_r(j) q_2^l(i+j, t) \right)^{Q_2-1}, \quad (17)$$

$$q_{p2}^l(j, t) = 1 - \left( 1 - \sum_{k=0}^{\infty} P_r(k) p_2^l(j-k, t) \right)^{A_2} \cdot (1 - p_{p2}^l(j, t)), \quad (18)$$

$$p_{p2}^{l+1}(j, t) = \epsilon \cdot q_{p2}^l(j, t). \quad (19)$$

In the first iteration, we have  $p_1^1(i, t) = p_{p1}^1(j, t) = p_2^1(i, t) = p_{p2}^1(j, t) = \epsilon$ . If  $A_1 = A_2 = A$ , we can derive  $q_1^1(j, t) = q_2^1(j, t)$  and  $q_{p1}^1(j, t) = q_{p2}^1(j, t)$  from (12), (16) and (14), (18), respectively. Consequently,  $p_1^2(i, t) = p_2^2(i, t)$  and  $p_{p1}^2(j, t) = p_{p2}^2(j, t)$ . In this case, for the later iterations, the DE equations for both the Type-1 and Type-2 connections can be simplified to

$$q_1^l(j, t) = q_2^l(j, t) = 1 - \left( 1 - \sum_{k=0}^{\infty} P_r(k) p_1^l(j-k, t) \right)^A \cdot (1 - p_{p1}^l(j, t))^2, \quad (20)$$

$$p_1^{l+1}(i, t) = p_2^{l+1}(i, t) = \epsilon \left( \sum_{j=0}^{t-i} P_r(j) q_1^l(i+j, t) \right)^{Q_1+Q_2-1}, \quad (21)$$

$$q_{p1}^l(j, t) = q_{p2}^l(j, t) = 1 - \left( 1 - \sum_{k=0}^{\infty} P_r(k) p_1^l(j-k, t) \right)^A$$

$$p_{p1}^{l+1}(j, t) = \epsilon \cdot q_{p1}^l(j, t) \cdot (1 - p_{p1}^l(j, t)),$$

As  $l \rightarrow \infty$ , we can rewrite the erasure probability of IN at position  $i$

$$P_e^{\text{BEC}}(i, t) = \epsilon \left\{ 1 - \sum_{j=0}^{t-i} P_r(j) \cdot \left[ \left( 1 - \sum_{k=0}^{\infty} P_r(k) p^\infty(i+j-k, t) \right)^{A-1} \cdot \left( 1 - p_p^\infty(i+j, t) \right)^2 \right]^{(Q_1+Q_2)} \right\}.$$

According to Lemma 1, the delay-exponent is derived as

$$\alpha_{\text{BEC}}(Q_1, Q_2, A_1, A_2, \lambda) = \lambda(Q_1 + Q_2). \quad (20)$$

whose value is exactly the same as that of the  $(Q, A, \lambda)$ -ensemble with  $Q = Q_1 + Q_2$ . ■

*Theorem 2: In a BI-AWGN channel, the RC Anytime  $(Q_1, Q_2, A_1, A_2, \lambda)$ -ensemble described in Definition 3 can achieve the same delay-exponent as the non-rate-compatible Anytime  $(Q_1 + Q_2, A, \lambda)$ -ensemble if  $A_1 = A_2 = A$ .*

The proof of the theorem can be found in Appendix C. It should be noted that, the non-rate-compatible Anytime  $(Q_1 + Q_2, A, \lambda)$ -ensemble is more randomized than the RC Anytime  $(Q_1, Q_2, A_1, A_2, \lambda)$ -ensemble, thus the results in Lemma 1 and Lemma 2 do not apply directly to the RC Anytime  $(Q_1, Q_2, A_1, A_2, \lambda)$ -ensemble.

Based on the above theorems and the remark given in Section III-A, we can conclude that the designed RC Anytime  $(Q_1, Q_2, A_1, A_2, \lambda)$ -ensemble can also achieve outstanding Anytime-reliable properties with guaranteed delay-exponents over both BEC and BI-AWGN channel, if the design condition  $A_1 = A_2 = A$  is satisfied.

### C. RC Anytime Code Family Construction

To construct an RC family, we start from an Anytime  $(Q_1, A_1, \lambda)$ -ensemble, i.e., the mother code ensemble, with a high design rate  $R_1 = \frac{A_1}{A_1+Q_1}$ . By successively adding new CNs and PNs to produce the  $(Q_n, Q_{n+1}, A_n, A_{n+1}, \lambda)$ -ensemble with  $A_{n+1} = A_n$ , where  $1 \leq n \leq N-1$ , we can construct a family of convolutional base matrices  $\mathbf{B} = \{\mathbf{B}_{[0,+\infty]}^1, \mathbf{B}_{[0,+\infty]}^2, \dots, \mathbf{B}_{[0,+\infty]}^N\}$  with design rates  $\mathbf{R} = \{R_1, R_2, \dots, R_N\}$ . We summarize this construction process in Algorithm 1 and provide an example in Fig. 3. Each square box in the figure represents a matrix.

As we defined earlier in Section III-A, the first three blocks of the mother code base matrix  $\mathbf{B}_{[0,2]}^1$  can be written as Fig. 3(a). To construct the first extended protograph,  $\mathbf{Z}_k^2$  is generated following the rules in line 7 of Algorithm 1. Then, according to lines 11 to 17, the first three blocks of the generated extended RC Anytime  $(Q_1, Q_2, A_1, A_2, \lambda)$ -ensemble i.e.,  $\mathbf{B}_{[0,2]}^2$ , are given as Fig. 3(b), where  $\mathbf{Z}_k^2$  with size  $b_c^2 \times b_v$  represents the edge connections from the  $b_v$  INs at position  $i$  to the  $b_c^2$  extended check nodes that are  $k$  positions away from it.

---

### Algorithm 1 Convolutional Base Matrix Construction of a Rate-Compatible Family of the Anytime $(Q, A, \lambda)$ -Ensemble

---

- 1: **Initialize**  $\mathbf{B}_k^1 = [\mathbf{Z}_k^1 \quad \mathbf{Z}_{\text{RA}}^1]$  for  $0 \leq k \leq t-1$  having information variable node degree  $Q_1$ , check node degree  $A_1$ , and design rate  $R_1 = \frac{A_1}{A_1+Q_1}$ .  $\mathbf{Z}_k^1$  have size  $b_c^1 \times b_v$ ,  $\mathbf{Z}_{\text{RA}}^1$  have size  $b_c^1 \times b_c^1$ .
  - 2: **for**  $n = 1 : N-1$  **do**
  - 3:   Use  $\mathbf{B}_k^n$  as the mother base matrix.
  - 4:   **for**  $k = 0 : t-1$  **do**
  - 5:     Set  $A_{n+1} = A_1$  and  $Q_{n+1}$ .
  - 6:     Set  $b_c^{n+1} = \frac{Q_{n+1}}{A_{n+1}} b_v$ .
  - 7:     Generate a full rank matrix  $\mathbf{Z}_k^{n+1}$  with size  $b_c^{n+1} \times b_v$  using the following rules:
    - 8:       1. The probability that there is a 1 in each row and in each column is  $Pr(k)$ .
    - 9:       2. The number of 1s in each row of  $\sum_{k=0}^{t-1} \mathbf{Z}_k^{n+1}$  equals to  $A_{n+1}$ .
    - 10:       3. The number of 1s in each column of  $\sum_{k=0}^{t-1} \mathbf{Z}_k^{n+1}$  equals to  $Q_{n+1}$ .
  - 11:     **if**  $k = 0$  **then**
  - 12:       Generate an RA matrix  $\mathbf{Z}_{\text{RA}}^{n+1}$  with size  $\sum_{i=1}^{n+1} b_c^i \times \sum_{i=1}^{n+1} b_c^i$ .
  - 13:       Form the extended base matrix as
 
$$\mathbf{B}_k^{n+1} = \begin{bmatrix} \mathbf{Z}_k^n & \\ & \mathbf{Z}_{\text{RA}}^{n+1} \end{bmatrix}$$
  - 14:     **else**
  - 15:       Generate an all-zero matrix  $\mathbf{0}^n$  with size  $\sum_{i=1}^{n+1} b_c^i \times \sum_{i=1}^{n+1} b_c^i$ .
  - 16:       Form the extended base matrix as
 
$$\mathbf{B}_k^{n+1} = \begin{bmatrix} \mathbf{Z}_k^n & \\ & \mathbf{0}^{n+1} \end{bmatrix}$$
  - 17:     **end if**
  - 18:   **end for**
  - 19:    $R_{n+1} = \frac{A_1}{A_1 + \sum_{i=1}^{n+1} Q_i}$ .
  - 20:    $n \leftarrow n + 1$ .
  - 21: **end for**
- 

$\mathbf{Z}_{\text{RA}}^2$  and  $\mathbf{0}^2$  are enlarged RA connection and enlarged all-zero matrix, respectively, now with the size of  $(b_c^1 + b_c^2) \times (b_c^1 + b_c^2)$ .

Finally, by performing the lifting operation on each of the element base matrices in the family, we can get a set of parity-check matrices  $\mathbf{H} = \{\mathbf{H}_{[0,+\infty]}^1, \mathbf{H}_{[0,+\infty]}^2, \dots, \mathbf{H}_{[0,+\infty]}^N\}$  with  $N$  different design rates, which is called as the RC Anytime code family.

*Lemma 4: The RC Anytime code family can cover the entire range of design rate  $R \in (0, 1)$ .*

*Proof:* In Algorithm 1, when  $n = 1$ , we have  $R_1 = \frac{A_1}{A_1+Q_1}$ , hence when  $Q_1 \rightarrow 0$ , we can derive  $R_1 \rightarrow 1$ ; when  $n = N-1$ , we can derive  $R_N = \frac{A_1}{A_1 + \sum_{i=1}^N Q_i}$  using Lemma 3, hence when  $\sum_{i=1}^N Q_i \rightarrow \infty$ , we can get  $R_N \rightarrow 0$ . ■

*Proposition 1: For both BEC and BI-AWGN channel, all the member codes in the designed RC Anytime code family have guaranteed good Anytime-reliable properties.*

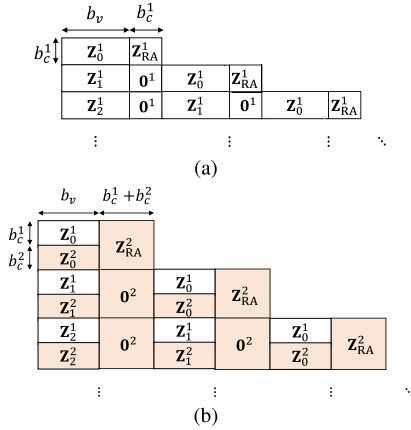


Fig. 3. First three blocks of the base matrix corresponding to the coupled-protograph of: (a) an Anytime  $(Q_1, A_1, \lambda)$ -ensemble with design rate  $R_1 = \frac{A_1}{A_1+Q_1}$ , (b) an extended RC Anytime  $(Q_1, Q_2, A_1, A_2, \lambda)$ -ensemble with a lower design rate  $R_2 = \frac{A_1}{A_1+Q_1+Q_2}$ . The extended matrices are shaded in orange.

*Proof:* According to Algorithm 1, for a given mother  $(Q_1, A, \lambda)$ -ensemble with a delay-exponent  $\alpha_{\text{BEC}} = \lambda Q_1$  (Lemma 1), we can extend it to a  $(Q_1, Q_e, A, A_e, \lambda)$ -ensemble, where  $A_e = A$ . The resulting ensemble can be written as a  $(Q_2, A, \lambda)$ -ensemble, where  $Q_2 = Q_1 + Q_e$  (Definition 3), and it can be proved to have  $\alpha_{\text{BEC}} = \lambda Q_2$  (Theorem 1). This new ensemble is then treated as a new mother code and extended to a  $(Q_2, Q_e, A, A_e, \lambda)$ -ensemble with  $A_e = A$ , resulting in  $\alpha_{\text{BEC}} = \lambda(Q_2 + Q_e)$ . By repeating this process, we can generate a series of rate-compatible Anytime code ensembles, where the  $n^{\text{th}}$  extended  $(Q_n, Q_{n+1}, A_n, A_{n+1}, \lambda)$ -ensemble can be written as  $(Q_n + Q_{n+1}, A, \lambda)$ -ensemble with a delay-exponent  $\alpha_{\text{BEC}} = \lambda(Q_n + Q_{n+1})$ . The proving process for BI-AWGN channels is similar, and the resulting  $(Q_n, Q_{n+1}, A_n, A_{n+1}, \lambda)$ -ensemble will have  $\alpha_{\text{BEC}}(\text{AWGN}) = 0.175\lambda(Q_n + Q_{n+1})$ . Therefore, every code ensemble within the family has been proven to have large delay-exponent over BEC and BI-AWGN channels. ■

#### D. Expanding-Window IR-HARQ Scheme

As we mentioned in Section I, the IR-HARQ scheme is a common application of the RC codes. However, we notice that the conventional IR-HARQ scheme [16] is unsuitable for Anytime codes. In the Anytime-coded transmission, if block  $\mathbf{x}_t$  can not be correctly decoded at the receiver at time  $t$ , it still has an opportunity to be corrected when the subsequent blocks  $\mathbf{x}_{t+1}, \mathbf{x}_{t+2}, \dots$  are received, then decoded together with  $\mathbf{x}_t$  by utilizing the expanding-window decoding [8]. Unfortunately, the conventional IR-HARQ scheme does not consider this expanded (delayed) decoding opportunity, i.e., if  $\mathbf{x}_t$  is detected to have error after decoding, the transmitter will be notified immediately through the feedback channel to send extra parity bits for  $\mathbf{x}_t$ , holding the transmission of the next block  $\mathbf{x}_{t+1}$ . Such a scheme is clearly wasteful and inefficient for the Anytime-coded transmission. In this regard, we modify the conventional IR-HARQ scheme and conceive a novel counterpart for the proposed RC Anytime codes, referred to as *expanding-window IR-HARQ scheme*.

The key to the design of the expanding-window IR-HARQ scheme is setting up a decoding delay (decoding window size) threshold  $d_{\text{th}}$ . Since the Anytime codes use the expanding window decoder, only when a block can not be decoded correctly<sup>4</sup> after its decoding window size meets the threshold  $d_{\text{th}}$ , the transmitter will be notified to transmit extra parity bits (the IR bits) for that block. Otherwise, the transmitter will continue to send the following blocks.

In this paper, we determine  $d_{\text{th}}$  using the delay-exponent of the highest-rate element code in the proposed RC Anytime SC-RA codes family. This configuration can ensure a good decoding performance for all codes within the family. We define the delay threshold  $d_{\text{th}}$  as<sup>5</sup>

$$d_{\text{th}} = - \left\lceil \frac{\log_{10} P_{e(\text{target})}}{\alpha_o} \right\rceil, \quad (21)$$

where  $P_{e(\text{target})}$  is the target decoding bit erasure/error rate, and  $\alpha_o$  is the *operational delay-exponent* which considers a finite  $d$  and binary phase shift keying (BPSK) modulation

$$\alpha_o = - \frac{\log_2 P_{e(\text{min})}^{\text{BEC or AWGN}}}{d}. \quad (22)$$

In (22),  $P_{e(\text{min})}$  is the asymptotic decoding erasure/error probability of the highest-rate element code (i.e., having the minimum variable node degree  $Q_{\text{min}}$ )

$$P_{e(\text{min})}^{\text{BEC}} = \epsilon \cdot e^{-\lambda Q_{\text{min}}(d+1)}, \quad (23)$$

$$P_{e(\text{min})}^{\text{AWGN}} = Q_f \left( \sqrt{\frac{N'_{\text{min}}}{2}} \right), \quad (24)$$

where  $N'_{\text{min}} = \frac{2}{\sigma_n^2} + 0.7\lambda Q_{\text{min}}(d+1) + 2.42Q_{\text{min}} - 1.75Q_{\text{min}}e^{-\lambda(d+1)}$ . The derivation of  $N'_{\text{min}}$  can be found in Appendix B. By setting  $d$  to a very large number (e.g.  $d = 100$ ), we can derive an  $\alpha_o$  whose value is close to the asymptotic  $\alpha$ . For example, in a BEC with  $\epsilon = 0.1$ , an RC Anytime SC-RA codes family with  $Q_{\text{min}} = 1$  has  $\alpha_o = 0.18$ , which is calculated from (22) and (23) by selecting  $d = 100$ . Then, using (21) we derive  $d_{\text{th}} = 22$  by selecting a target bit erasure rate  $P_{e(\text{target})} = 10^{-4}$ .

After determining  $d_{\text{th}}$ , we propose the expanding-window IR-HARQ scheme in Algorithm 2, where  $s$  denotes the target block index that is used to track whether the decoding window threshold has been reached by block  $\mathbf{x}_s$ , and  $n$  denotes the index of the element parity-check matrix in the RC family  $\mathbf{H}_{[0,+\infty]}^n$ ,  $n \in [1, N]$ .

## IV. NUMERICAL RESULTS

In this section, we present simulation results of the proposed RC Anytime SC-RA codes and their applications in the ARQ scenarios when used with the proposed expanding-window IR-HARQ scheme. Note that the reliability of anytime coding hinges on the performance of each individual block within an

<sup>4</sup>In BEC, a block cannot be decoded correctly means the block still contains erased bits. In BI-AWGN channel, it means the cyclic redundancy check fails.

<sup>5</sup>Here we briefly explain the idea. Recalling from Section II that  $-\alpha$  represents the slope of the asymptotic  $P_e$  curve versus  $d$ . As a result, we can calculate the comparable required  $d$ , using  $\alpha$ , for any achievable  $P_{e(\text{target})}$  level.

---

**Algorithm 2** Anytime IR-HARQ Scheme
 

---

```

1: Input  $\mathbf{H} = \{\mathbf{H}_{[0,+\infty]}^1, \dots, \mathbf{H}_{[0,+\infty]}^N\}$ ,  $d_{\text{th}}$ 
2: Initialize  $s \leftarrow 0$ ,  $n \leftarrow 1$ 
3: while  $t \geq 0$  do
Transmitter Side:
4:   if  $t - s < d_{\text{th}}$  then
5:     Use  $\mathbf{H}_{[0,t]}^1$  to generate codeword  $\mathbf{x}_t^1 = [m_t, p_t^1]$ 
     and send  $\mathbf{x}_t^1$ 
6:   else if  $t - s == d_{\text{th}}$  then
7:     Use  $\mathbf{H}_{[0,s]}^n$  to generate IR bits  $p_s^n$  for block  $\mathbf{x}_s$  and
     send  $p_s^n$ 
8:   end if
Receiver Side:
9:   Use  $\mathbf{H}_{[0,t]}^n$  to decode  $\bar{\mathbf{x}}_{[0,t]}^n$  and generate estimated
   message  $\hat{m}_s$ 
10:  if  $\hat{m}_s$  is correctly decoded then
11:    Send ACK for block  $s$  to the transmitter
12:     $s \leftarrow s + 1$ ,  $n \leftarrow 1$ ,  $t \leftarrow t + 1$ 
13:  else
14:    if  $t - s < d_{\text{th}}$  then
15:       $t \leftarrow t + 1$ 
16:    else if  $t - s == d_{\text{th}}$  then
17:      if  $n = N$  then
18:         $s \leftarrow s + 1$ ,  $n \leftarrow 1$ ,  $t \leftarrow t + 1$ 
19:      else if  $n < N$  then
20:         $n \leftarrow n + 1$ 
21:      end if
22:    end if
23:  end if
24: end while
    
```

---

anytime-code sequence, whose  $L$  continually lengthens as  $d$  increases. Consequently, our simulation results in Fig. 4-6 and 8-10 concentrate on the decoding performances of block  $\mathbf{x}_1$  of Anytime codes.

### A. Performance Over BEC

First of all, in order to verify the correctness of Table I, we present in Fig. 4 the finite-length bit-erasure rate curves (solid lines) of the Anytime code ensembles listed in Table I, with the lifting factor set to 50 for all codes. The asymptotic performances (dashed lines), which reflect the theoretical delay-exponent, are also included in the figure as benchmarks. We observe that the decreasing trends of all finite-length curves are consistent with their asymptotic curves. Among the Anytime code ensembles, the Anytime SC-RA (6, 6, 0.5)-ensemble, which has the highest delay-exponent value, shows the fastest bit-erasure rate reduction. These results confirm the accuracy of Lemma 1 and Table I.

We then construct an RC family with design rate  $R \in \{2/3, 1/2, 1/3, 1/4\}$  from an Anytime (4, 4, 0.1)-ensemble and compare it with the only RC Anytime code family reported in the literature [9]. The simulation results are shown in Fig. 5, where both RC families are with lifting factor  $M = 3$  and transmitted over a BEC with channel erasure rate  $\epsilon = 0.3$ . Both families are set to have chain length  $L = 50$  and coupling

width  $w = 50$ , so that the block lengths are of  $\{4, 6, 9, 12\}$  and the maximum codeword lengths are of  $\{200, 300, 450, 600\}$ . If the entire codeword is transmitted and decoded successfully, the total information length should be 150 bits. The bit-erasure rate curves of the non-rate-compatible (non-RC) Anytime SC-RA codes with the same parameters are also plotted in the figure. It can be seen that the decoding performance curves of the proposed RC Anytime codes, at all three code rates, agree well with the non-RC ones (which confirms Theorem 1 and Proposition 1). When compared with the RC Anytime codes of [9], our proposed RC Anytime SC-RA codes show similar bit-erasure rate decaying speeds (i.e., similar delay-exponent values) and are observed to achieve much lower erasure floors due to the low-density structure of the parity-check matrix.

Apart from the superior decoding performance, our proposed RC family also shows a great advantage in the designable code rate range: our RC Anytime codes may take any rational design rate in the range of 0 to 1, while the RC Anytime codes in [9] can only have a design rate of  $1/r$ , where  $r \geq 2$  (e.g.,  $1/2, 1/3, 1/4, \dots$ ).

Note that in Fig. 5, the proposed RC anytime codes family, with design rates  $R \in \{2/3, 1/2, 1/3, 1/4\}$  and parameters  $L = 50$  and  $w = 50$ , has actual code rates of  $\{0.4926, 0.3268, 0.1953, 0.1393\}$  for the entire codeword as calculated from equation (5). This significant rate loss resulted from the large number of additional check nodes appended at the end of the chain due to the large value of  $w$ . However, as our focus is on the performance of each individual block of Anytime codes and we employ an expanding-window decoding scheme [8] that truncates additional check nodes within each window, the effective code rates in our simulations remain  $\{2/3, 1/2, 1/3, 1/4\}$ .

Now we simulate our proposed RC Anytime code family in the HARQ communication scenario. Fig. 6 illustrates the performance of the proposed RC Anytime codes with an average code rate of  $\bar{R} = 0.3918$  (measured over 100 blocks), implemented with the proposed expanding-window IR-HARQ scheme using  $d_{\text{th}} = 9$  for a target bit-erasure rate of  $10^{-3}$ . In addition, we evaluate the performance of the RC Anytime codes from [9] using both their own IR-HARQ scheme and our proposed scheme at an average code rate of  $\bar{R} = 0.38$ . Our results show that the proposed RC Anytime SC-RA codes, when used with our proposed IR-HARQ scheme, exhibit excellent bit-erasure correction capabilities, with the bit-erasure rate decaying rapidly down to  $10^{-5}$ . On the other hand, the bit-erasure rate of the RC Anytime codes from [9] decays much slower and has a lower average code rate when run with either of the IR-HARQ schemes. This suboptimal performance is mainly due to the high erasure floor of the codes at every code rate, as shown in Fig. 5.

Moreover, in Fig. 7 we compare the performance of the proposed RC Anytime codes family with the RC (non-Anytime) LDPC codes family [31] in the HARQ communication systems. The performance metric employed here is the cumulative number of Correctly Decoded Information bits (CDI) as a function of the decoding delay. The information block length for the RC Anytime SC-RA codes and the RC LDPC codes are set as 20-bit and 512-bit, respectively. It can be observed from

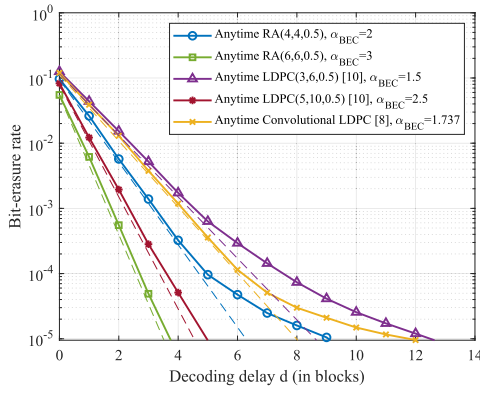


Fig. 4. Finite-length decoding results (solid lines) with  $M = 50$  and asymptotic performances (dashed lines) of different Anytime codes (block  $x_1$ ) transmitted over BEC with  $\epsilon = 0.3$ .

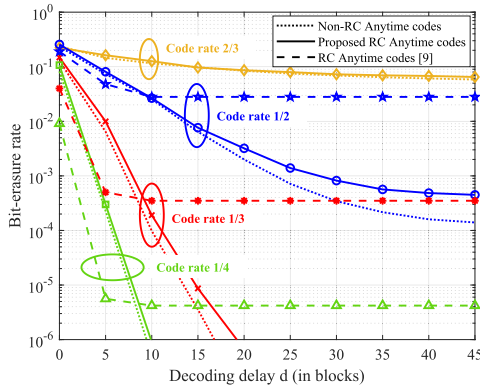


Fig. 5. Decoding performance of block  $x_1$  of the non-RC Anytime SC-RA codes (dotted lines), the proposed RC Anytime SC-RA codes (solid line) and the existing RC Anytime codes [9] (dashed line), both with  $M = 3$ , over a BEC ( $\epsilon = 0.3$ ).

Fig. 7 that the CDI of the proposed RC Anytime codes, using either the conventional IR-HARQ scheme or the proposed expanding-window IR-HARQ scheme, improves with every increment of decoding delay (decoding window size), right from the beginning of the transmission, while for the RC LDPC codes [31], the CDI can only be acquired when the entire long codeword block has been decoded. Furthermore, when the RC Anytime SC-RA codes employ the proposed expanding-window IR-HARQ scheme, we can observe a much better CDI performance than that using the conventional IR-HARQ scheme at all decoding delays.

### B. Performance Over BI-AWGN Channel

For the BI-AWGN channel, Fig. 8 displays the bit-error rate curves for the two Anytime code ensembles listed in Table II with  $M = 12$ . The solid lines correspond to  $\text{SNR}=0.5\text{dB}$ , while the dotted lines correspond to  $\text{SNR}=2\text{dB}$ . As the lower bound delay-exponent values cannot fully describe the asymptotic decoding performance, we have not provided the asymptotic results in the figure. Nonetheless, we can still observe that the Anytime RA code ensemble with higher  $\underline{\alpha}_{\text{AWGN}}$  achieves better performance than the Anytime convolutional codes with lower  $\underline{\alpha}_{\text{AWGN}}$  over both BI-AWGN channels.

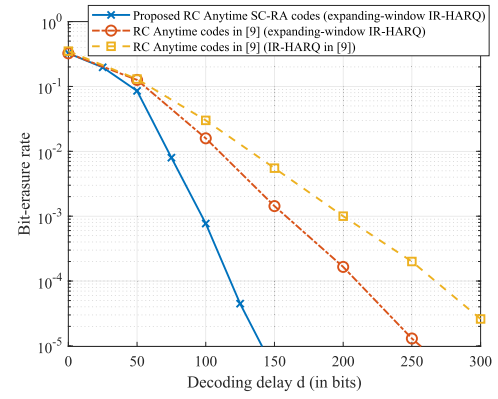


Fig. 6. Bit-erasure correction performance of block  $x_1$  of the proposed RC Anytime SC-RA codes and the existing RC Anytime convolutional LDPC codes [9] in a HARQ communication system with  $M = 5$  over a BEC ( $\epsilon = 0.5$ ).

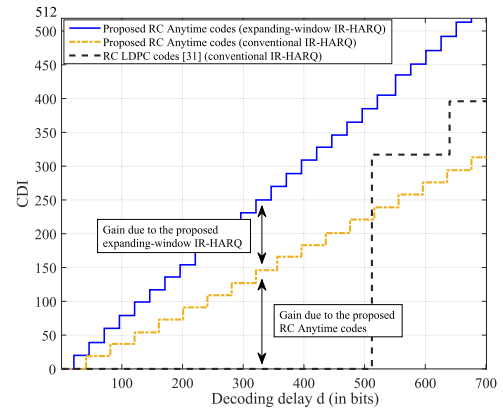


Fig. 7. Cumulative number of correctly decoded information bits (CDI) of the proposed RC Anytime codes with the proposed expanding-window IR-HARQ scheme, compared with the conventional (Non-Anytime) RC LDPC codes with conventional IR-HARQ scheme over a BEC ( $\epsilon = 0.1$ ).

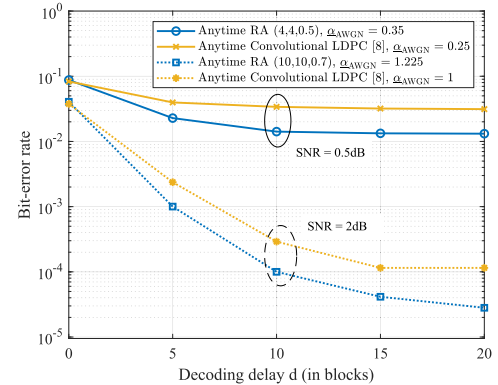


Fig. 8. Bit-error correction performance of different Anytime codes (block  $x_1$ ) with  $M = 12$  transmitted over BI-AWGN channels.

Fig. 9 shows the finite-length decoding performance of the proposed RC Anytime SC-RA codes and non-RC Anytime SC-RA codes with four different design rates  $R \in \{2/3, 1/2, 1/3, 1/4\}$ . We set  $L = 50$ ,  $w = 50$ , and  $M = 10$ , resulting in block lengths of  $\{15, 20, 30, 40\}$  and maximum codeword lengths of  $\{750, 1000, 1500, 2000\}$ . The maximum information length is 500 bits. Since there are no prior-art RC Anytime codes designed for the BI-AWGN channel to

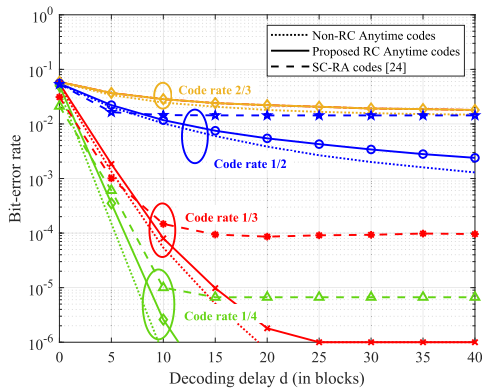


Fig. 9. Decoding performance of block  $x_1$  of the non-RC Anytime SC-RA codes (dotted lines), the proposed RC Anytime SC-RA codes (solid lines) and the (non-Anytime) SC-RA codes [24] (dashed lines) with  $M = 10$  over a BI-AWGN channel (SNR = 1dB).

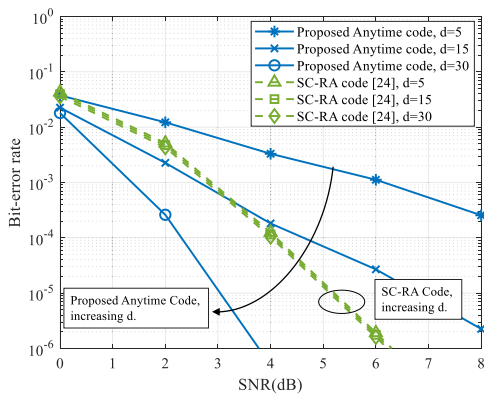


Fig. 10. Decoding performance of block  $x_1$  of the proposed RC Anytime codes and the (non-Anytime) SC-RA codes [24] with rate-1/2 and  $M = 10$  over BI-AWGN channels.

compare with, here we also include the finite-length performance of (non-Anytime) SC-RA codes [24] of the same block length and code rates. As expected, the (non-Anytime) SC-RA codes present high error floors at all three code rates due to their small coupling length. In contrast, the RC Anytime SC-RA codes show a continuous error-correction trend similar to that of the non-RC performance curves as  $d$  increases. This observation supports Theorem 2 and Proposition 1.

Furthermore, Fig. 10 shows the bit-error rate performance of the two codes with code rate-1/2 for different SNR values at various  $d$ . At all SNR values, the proposed Anytime code is observed to have its decoding bit-error rate improves with the increasing decoding delay (i.e., the increasing decoding window size), while the (non-Anytime) SC-RA code gains little from this decoding window size expansion. Codes with other code rates also show a similar trend.

In Fig. 11, considering the application in the HARQ systems, we compare the CDI performance of the proposed RC Anytime code family, the RC irregular RA (IRA) codes family [18], and the RC Polar codes family [32]. The proposed RC Anytime SC-RA codes with information block length of 20-bit employ the expanding-window IR-HARQ scheme and the conventional IR-HARQ scheme, respectively, where the

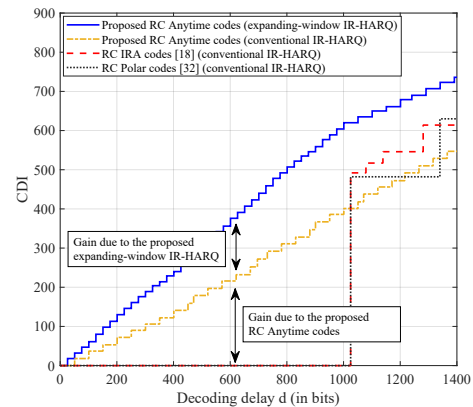


Fig. 11. CDI performance benchmarking for the proposed RC Anytime codes used with the proposed expanding-window IR-HARQ scheme over BI-AWGN channel (SNR = -2dB).

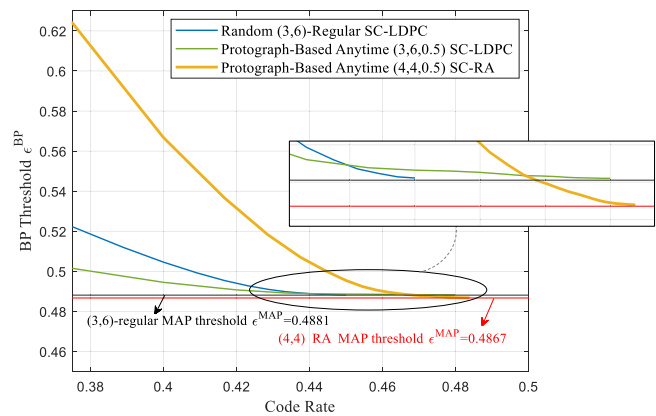


Fig. 12. BEC BP decoding threshold for three code ensembles. Also shown are the MAP decoding thresholds for the underlying (3, 6)-regular LDPC ensemble and (4, 4) RA ensemble,  $\epsilon^{MAP} = 0.4881$  and  $\epsilon^{MAP} = 0.4867$ , respectively.

expanding-window IR-HARQ scheme is set to have  $d_{th} = 26$  for  $P_{e(target)} = 10^{-3}$ .

The RC IRA codes [18] and the RC Polar codes [32], both using the conventional IR-HARQ scheme, assume the information block length is 1024 bits. As observed, the CDI of our proposed RC Anytime code family, using the expanding-window IR-HARQ scheme, improves with every increment of decoding delay (decoding window size), right from the beginning of the transmission, and can achieve the largest value at every decoding delay.

## V. CONCLUSION

In this paper, we design and construct a new RC Anytime code family based on SC-RA codes. We first introduce an Anytime SC-RA code (Anytime  $(Q, A, \lambda)$ -ensemble) as the mother code. By analyzing its delay-exponent, we show that the Anytime  $(Q, A, \lambda)$ -ensemble has outstanding Anytime-reliable properties over both BEC and BI-AWGN channel with a simple code structure. Then, we apply protograph extension on this mother code to design a rate-compatible Anytime  $(Q_1, Q_2, A_1, A_2, \lambda)$ -ensemble with guaranteed delay-exponent as good as non-rate-compatible Anytime  $(Q, A, \lambda)$ -ensemble of the same design rate. Furthermore, we put forward an

expanding-window IR-HARQ scheme to make use of the proposed RC Anytime SC-RA codes in ARQ communication systems. Simulated results indicate that the proposed RC Anytime SC-RA codes are superior to the prior-art RC Anytime codes in terms of the decoding performance, due to better control of their parity-check density. In addition, over both BEC and BI-AWGN channel, the proposed RC Anytime SC-RA codes family combined with the proposed expanding-window IR-HARQ scheme has the advantage of fast and continuous accumulation of CDI bits at the receiver even with short decoding delays, while the conventional non-Anytime RC error correction codes can only achieve stepwise improvement of CDI. These benefits are crucial in noisy control systems and can play an essential role in delay-sensitive applications such as those envisaged by the ultra-reliable low latency communications (URLLC) defined in the 5G wireless standard. As a future direction, we plan to analyze the error floor problem that arises in finite-length Anytime codes, with the aim of further enhancing the code. Additionally, it would be interesting to investigate other distributions of coupling connections that exhibit Anytime-reliable properties and offer improved performance.

#### APPENDIX A

##### NUMERICAL EVIDENCE OF ANYTIME CODES' THRESHOLD SATURATION PROPERTY

The threshold saturation property has been rigorously proven for random SC-LDPC codes [25] and numerically supported for random SC-RA codes, protograph-based SC-LDPC codes, and protograph-based SC-RA codes by [24], [26], and [27], respectively.

Here we numerically show that the Anytime SC-RA codes exhibit threshold saturation property. In Fig. A1, we present the BP decoding threshold  $\epsilon^{\text{BP}}$  of three code ensembles: the uniformly-distributed random SC-LDPC, the exponentially-distributed protograph-based Anytime SC-LDPC, and the exponentially-distributed protograph-based Anytime SC-RA, in terms of their design rates. Both of the exponentially-distributed codes are with  $w = 10$  and  $\lambda = 0.5$ . It can be observed that as the code rate increases (i.e., as  $L$  increases),  $\epsilon^{\text{BP}}$  of all three code ensembles converge to the MAP threshold of their underlying LDPC or RA codes, although the exponentially-distributed Anytime codes converge much slower than the uniformly-distributed codes. This observation provides numerical verification that both the Anytime SC-LDPC codes and the Anytime SC-RA codes indeed possess the threshold saturation property.

#### APPENDIX B PROOF OF LEMMA 2

To simplify the proof for the BI-AWGN channel, we employ the Gaussian approximation (GA) technique [29], where the LLR messages with  $N(\mu, \sigma^2)$  satisfy  $\sigma^2 = 2\mu$ . In the  $l$ -th iteration at time  $t$ , we define  $\bar{x}^l(i, t)$  and  $\bar{x}_p^l(j, t)$  as the mean values of LLR messages sent from an IN at position  $i$  and from a PN at position  $j$ , respectively; we also define  $\bar{y}^l(j, t)$  and  $\bar{y}_p^l(j, t)$  as the mean values of LLR messages sent from

a CN at position  $j$  to an IN and to a PN, respectively. For a given channel noise variance  $\sigma_n^2$ , we initialize  $\bar{x}^0(i, t) = \bar{x}_p^0(j, t) = \frac{2}{\sigma_n^2}$  for  $0 < i, j \leq t$ . The approximated DE equations are given as (25)-(28), shown at the top of the next page, where  $\phi(u) = 1 - \frac{1}{\sqrt{4\pi u}} \int_{-\infty}^{\infty} (\tanh \frac{f}{2}) e^{-\frac{(f-u)^2}{4u}} df$  and  $J(u) = 1 - \frac{1}{\sqrt{4\pi u}} \int_{-\infty}^{\infty} e^{-\frac{(f-u)^2}{4u}} \log_2(1 + e^{-f}) df$ . Therefore, the error probability of IN at position  $i$  after an infinite number of iterations is

$$P_e^{\text{AWGN}}(i, t) = \mathcal{Q}_f \left( \sqrt{\frac{X(i, t)}{2}} \right), \quad (29)$$

where  $\mathcal{Q}_f(\cdot)$  is the Q-function, and

$$X(i, t) = \frac{2}{\sigma_n^2} + Q \cdot J^{-1} \left( \sum_{j=0}^{t-i} P_r(j) J(y^\infty(i+j, t)) \right). \quad (30)$$

Similar to the proof of Lemma 1, we use the fact that the threshold saturation phenomenon of protograph-based SC-LDPC codes (and therefore protograph-based SC-RA codes) was numerically observed to hold for binary-input, memoryless, output-symmetric (BMS) channels [26]. Thus, for  $\sigma_n \leq \sigma_n^{\text{MAP}}(Q, A)$ , where  $\sigma_n^{\text{MAP}}(Q, A)$  is the MAP threshold of the underlying RA protograph  $(Q, A)$ -ensemble over BI-AWGN channel, the mean values of LLR messages from an IN (or a PN) will approach infinity after an infinite number of iterations. Therefore, for  $\sigma_n \leq \sigma_n^{\text{MAP}}(Q, A)$ , we apply  $x^\infty(i, t) = \infty$  and  $x_p^\infty(i, t) = \infty$  to (25)-(30) and obtain

$$\begin{aligned} \lim_{t \rightarrow \infty} y^l(j, t) &= \phi^{-1} \left\{ 1 - \left[ 1 - \phi \left( J^{-1} \left( \sum_{k=0}^{\infty} P_r(k) \cdot 1 \right) \right) \right]^{A-1} \right. \\ &\quad \left. \cdot [1 - 0]^2 \right\} \\ &= \phi^{-1} \left\{ 1 - [1 - 0]^{A-1} [1 - 0]^2 \right\} \\ &= \infty. \end{aligned} \quad (31)$$

Here we employ the facts that  $\phi(u)$  is continuous and monotonically decreasing on  $[0, \infty)$ , with  $\phi(0) = 1$  and  $\phi(\infty) = 0$ ;  $J(u)$  is continuous and monotonically increasing on  $[0, \infty)$ , with  $J(0) = 0$  and  $J(\infty) = 1$ .

Applying (31) into (30), we have

$$\begin{aligned} X(i, t) &= \frac{2}{\sigma_n^2} + Q J^{-1} \left( \sum_{j=0}^d P_r(j) \cdot 1 \right) \\ &\stackrel{(a)}{=} \frac{2}{\sigma_n^2} + Q J^{-1} (1 - e^{-\lambda(d+1)}) \\ &\stackrel{(b)}{\approx} \frac{2}{\sigma_n^2} + Q \left[ -0.7 \log_e \left( 0.386 e^{-\lambda(d+1)} \right) \right. \\ &\quad \left. + 1.75 \left( 1 - e^{-\lambda(d+1)} \right) \right] \end{aligned}$$

$$\bar{y}^l(j, t) = \phi^{-1} \left\{ 1 - \left[ 1 - \phi \left( J^{-1} \left( \sum_{k=0}^{\infty} P_r(k) J(\bar{x}^l(j-k, t)) \right) \right) \right]^{A-1} \cdot [1 - \phi(\bar{x}_p^l(j, t))]^2 \right\}, \quad (25)$$

$$\bar{x}^{l+1}(i, t) = \frac{2}{\sigma_n^2} + (Q-1)J^{-1} \left( \sum_{j=0}^{t-i} P_r(j) J(\bar{y}^l(i+j, t)) \right), \quad (26)$$

$$\bar{y}_p^l(j, t) = \phi^{-1} \left\{ 1 - \left[ 1 - \phi \left( J^{-1} \left( \sum_{k=0}^{\infty} P_r(k) J(\bar{x}^l(j-k, t)) \right) \right) \right]^A \cdot [1 - \phi(\bar{x}_p^l(j, t))] \right\}, \quad (27)$$

$$\bar{x}_p^{l+1}(j, t) = \frac{2}{\sigma_n^2} + \bar{y}_p^l(j, t). \quad (28)$$

$$\approx \frac{2}{\sigma_n^2} + 0.7\lambda Q(d+1) + 2.42Q - 1.75Qe^{-\lambda(d+1)}, \quad (32)$$

where in (a) we apply (4) to  $P_r(j)$ , and in (b) we use the approximation of  $J^{-1}(u)$  from [30]. Thus, by replacing (32) into (29), we can derive

$$P_e^{\text{AWGN}}(i, t) = \mathcal{Q}_f \left( \sqrt{\frac{N'}{2}} \right), \quad (33)$$

where  $N' = \frac{2}{\sigma_n^2} + 0.7\lambda Q(d+1) + 2.42Q - 1.75Qe^{-\lambda(d+1)}$ . The exact value of the delay-exponent can then be obtained by replacing (33) into (2)

$$\alpha_{\text{AWGN}}(Q, A, \lambda) \triangleq \lim_{d \rightarrow \infty} \left( \lim_{i \rightarrow \infty} - \left( \frac{\log \mathcal{Q}_f \left( \sqrt{\frac{N'}{2}} \right)}{d} \right) \right). \quad (34)$$

Here, to show the relationship between  $\alpha_{\text{AWGN}}$ ,  $\lambda$ , and  $Q$  in a clear manner, we also derive the lower bound for  $\alpha_{\text{AWGN}}$ . Using the fact that  $\mathcal{Q}_f(u) \leq e^{-\frac{u^2}{2}}$  for  $u \geq 0$ , we have

$$\lim_{l \rightarrow \infty} P_e^{\text{AWGN}}(i, t) \leq e^{-\left(\frac{X(i,t)}{4}\right)} = e^{-(0.175\lambda Q(d+1)+Z')},$$

where  $Z' = \frac{1}{2\sigma_n^2} + 0.605Q - 0.4375Qe^{-\lambda(d+1)}$ . According to (33) and (34), we can obtain

$$\alpha_{\text{AWGN}}(Q, A, \lambda) \geq 0.175\lambda Q.$$

#### APPENDIX C PROOF OF THEOREM 2

For DE analysis of the Anytime  $(Q_1, Q_2, A_1, A_2, \lambda)$ -ensemble, in the  $l$ -th iteration at time  $t$ , we define  $x_1^l(i, t)$  (or  $x_2^l(i, t)$ ) and  $x_{p1}^l(j, t)$  (or  $x_{p2}^l(j, t)$ ) to be the pdf for the LLR message sent from an IN at position  $i$  and a PN at position  $j$  to the Type-1 CN<sub>1</sub> (or Type-2 CN<sub>2</sub>), respectively;  $y_1^l(j, t)$  (or  $y_2^l(j, t)$ ) and  $y_{p1}^l(j, t)$  (or  $y_{p2}^l(j, t)$ ) to be the pdf for the LLR message sent from a Type-1 CN<sub>1</sub> (or Type-2 CN<sub>2</sub>) at position  $j$  to an IN and to a PN, respectively. For a given channel pdf  $a$ , the DE equations of the Type-1 (or Type-2) connection are written as

$$y_{1(\text{or } 2)}^l(j, t) = \left( \sum_{k=0}^{\infty} P_r(k) x_{1(\text{or } 2)}^l(j-k, t) \right)^{\otimes (A_{1(\text{or } 2)}-1)}$$

$$\otimes x_{p1(\text{or } p2)}^l(j, t)^{\otimes 2},$$

$$x_{1(\text{or } 2)}^{l+1}(i, t) = a \otimes \left( \sum_{j=0}^{t-i} P_r(j) y_1^l(i+j, t) \right)^{\otimes (Q_1-1)(\text{or } Q_1)}$$

$$\otimes \left( \sum_{j=0}^{t-i} P_r(j) y_2^l(i+j, t) \right)^{\otimes Q_2(\text{or } (Q_2-1))},$$

$$y_{p1(\text{or } p2)}^l(j, t) = \left( \sum_{k=0}^{\infty} P_r(k) x_{1(\text{or } 2)}^l(j-k, t) \right)^{\otimes A_{1(\text{or } 2)}}$$

$$\otimes x_{p1(\text{or } p2)}^l(j, t),$$

$$x_{p1(\text{or } p2)}^{l+1}(j, t) = a \otimes y_{p1(\text{or } p2)}^l(j, t).$$

Similar to the proof of Theorem 1, we can rewrite the Type-1 and Type-2 DE recursions to get the following error probability of the IN at position  $i$  if  $A_1 = A_2 = A$

$$P_e^{\text{AWGN}}(i, t) = a \otimes \left\{ \sum_{j=0}^{t-i} P_r(j) \right.$$

$$\left. \otimes \left[ \left( \sum_{k=0}^{\infty} P_r(k) x^\infty(i+j-k, t) \right)^{\otimes (A-1)} \right. \right.$$

$$\left. \left. \otimes x_p^\infty(i+j, t)^{\otimes 2} \right] \right\}^{\otimes (Q_1+Q_2)}.$$

Then, the delay-exponent can be derived using a similar approach to that used in the proof of Lemma 2, which is exactly the same as that of the  $(Q, A, \lambda)$ -ensemble with  $Q = Q_1 + Q_2$ .

#### REFERENCES

- [1] A. Sahai, "Anytime information theory," Ph.D. dissertation, Dept. Elect. Eng. Comput. Sci., Massachusetts Inst. Technol., Cambridge, MA, USA, 2001.
- [2] A. Sahai and S. Mitter, "The necessity and sufficiency of anytime capacity for stabilization of a linear system over a noisy communication link—Part I: Scalar systems," *IEEE Trans. Inf. Theory*, vol. 52, no. 8, pp. 3369–3395, Aug. 2006.
- [3] L. Grosjean, "Practical anytime codes," Ph.D. dissertation, KTH School Elect. Eng., KTH Roy. Inst. Technol., Stockholm, Sweden, 2016.

- [4] R. T. Sukhavasi and B. Hassibi, "Linear error correcting codes with anytime reliability," in *Proc. IEEE Int. Symp. Inf. Theory*, Jul. 2011, pp. 1748–1752.
- [5] R. T. Sukhavasi and B. Hassibi, "Anytime reliable codes for stabilizing plants over erasure channels," in *Proc. IEEE Conf. Decis. Control Eur. Control Conf.*, Dec. 2011, pp. 5254–5259.
- [6] G. Como, F. Fagnani, and S. Zampieri, "Anytime reliable transmission of real-valued information through digital noisy channels," *SIAM J. Control Optim.*, vol. 48, no. 6, pp. 3903–3924, Jan. 2010.
- [7] A. Tarable, A. Nordio, F. Dabbene, and R. Tempo, "Anytime reliable LDPC convolutional codes for networked control over wireless channel," in *Proc. IEEE Int. Symp. Inf. Theory*, Jul. 2013, pp. 2064–2068.
- [8] L. Grosjean, L. K. Rasmussen, R. Thobaben, and M. Skoglund, "Systematic LDPC convolutional codes: Asymptotic and finite-length anytime properties," *IEEE Trans. Commun.*, vol. 62, no. 12, pp. 4165–4183, Dec. 2014.
- [9] L. Grosjean, R. Thobaben, L. K. Rasmussen, and M. Skoglund, "Variable-rate anytime transmission with feedback," in *Proc. IEEE 84th Veh. Technol. Conf. (VTC-Fall)*, Sep. 2016, pp. 1–6.
- [10] M. Noor-A-Rahim, K. D. Nguyen, and G. Lechner, "Anytime reliability of spatially coupled codes," *IEEE Trans. Commun.*, vol. 63, no. 4, pp. 1069–1080, Apr. 2015.
- [11] N. Zhang, M. Noor-A-Rahim, B. N. Vellambi, and K. D. Nguyen, "Anytime characteristics of protograph-based LDPC convolutional codes," *IEEE Trans. Commun.*, vol. 64, no. 10, pp. 4057–4069, Oct. 2016.
- [12] M. Noor-A-Rahim, M. O. Khyam, Y. L. Guan, G. G. M. N. Ali, K. D. Nguyen, and G. Lechner, "Delay-universal channel coding with feedback," *IEEE Access*, vol. 6, pp. 37918–37931, 2018.
- [13] L. Deng, Y. Wang, X. Yu, M. Noor-A-Rahim, Y. L. Guan, and Z. Shi, "Joint source channel anytime coding," in *Proc. GLOBECOM IEEE Global Commun. Conf.*, Dec. 2020, pp. 1–6.
- [14] M. Noor-A-Rahim, K. D. Nguyen, G. Lechner, and Y. L. Guan, "Design and analysis of anytime codes for relay channels," *IEEE Trans. Commun.*, vol. 66, no. 4, pp. 1349–1362, Apr. 2018.
- [15] A. Tarable and F. J. Escrivano, "Chaos-based anytime-reliable coded communications," *IEEE Syst. J.*, vol. 14, no. 2, pp. 2214–2224, Jun. 2020.
- [16] C. Sahin, L. Liu, E. Perrins, and L. Ma, "Delay-sensitive communications over IR-HARQ: Modulation, coding latency, and reliability," *IEEE J. Sel. Areas Commun.*, vol. 37, no. 4, pp. 749–764, Apr. 2019.
- [17] C.-H. Hsu and A. Anastasopoulos, "Capacity achieving LDPC codes through puncturing," *IEEE Trans. Inf. Theory*, vol. 54, no. 10, pp. 4698–4706, Oct. 2008.
- [18] G. Yue, X. Wang, and M. Madhian, "Design of rate-compatible irregular repeat accumulate codes," *IEEE Trans. Commun.*, vol. 55, no. 6, pp. 1153–1163, Jun. 2007.
- [19] N. Jacobsen and R. Soni, "Design of rate-compatible irregular LDPC codes based on edge growth and parity splitting," in *Proc. IEEE 66th Veh. Technol. Conf.*, Sep. 2007, pp. 1627–1631.
- [20] S. J. Johnson, *Iterative Error Correction: Turbo, Low-Density Parity-Check and Repeat-Accumulate Codes*. Cambridge, U.K.: Cambridge Univ. Press, 2010.
- [21] D. Divsalar, S. Dolinar, C. Jones, and K. Andrews, "Capacity-approaching protograph codes," *IEEE J. Sel. Areas Commun.*, vol. 27, no. 6, pp. 876–888, Aug. 2009.
- [22] A. E. Pusane, A. J. Feltstrom, A. Sridharan, M. Lentmaier, K. Zigangirov, and D. J. Costello, "Implementation aspects of LDPC convolutional codes," *IEEE Trans. Commun.*, vol. 56, no. 7, pp. 1060–1069, Jul. 2008.
- [23] T. J. Richardson and R. L. Urbanke, "The capacity of low-density parity-check codes under message-passing decoding," *IEEE Trans. Inf. Theory*, vol. 47, no. 2, pp. 599–618, Feb. 2001.
- [24] S. Johnson and G. Lechner, "Spatially coupled repeat-accumulate codes," *IEEE Commun. Lett.*, vol. 17, no. 2, pp. 373–376, Feb. 2013.
- [25] S. Kudekar, T. J. Richardson, and R. L. Urbanke, "Threshold saturation via spatial coupling: Why convolutional LDPC ensembles perform so well over the BEC," *IEEE Trans. Inf. Theory*, vol. 57, no. 2, pp. 803–834, Feb. 2011.
- [26] D. G. M. Mitchell, M. Lentmaier, and D. J. Costello, "Spatially coupled LDPC codes constructed from protographs," *IEEE Trans. Inf. Theory*, vol. 61, no. 9, pp. 4866–4889, Sep. 2015.
- [27] M. Stinner and P. M. Olmos, "On the waterfall performance of finite-length SC-LDPC codes constructed from protographs," *IEEE J. Sel. Areas Commun.*, vol. 34, no. 2, pp. 345–361, Feb. 2016.
- [28] S. Lin and D. J. Costello, *Error Control Coding: Fundamentals and Applications*, 2nd ed. Englewood Cliffs, NJ, USA: Prentice-Hall, 2004.
- [29] M. Noor-A-Rahim, G. Lechner, and K. D. Nguyen, "Density evolution analysis of spatially coupled LDPC codes over BIAWGN channel," in *Proc. Austral. Commun. Theory Workshop (AusCTW)*, Jan. 2016, pp. 13–17.
- [30] S. ten Brink, G. Kramer, and A. Ashikhmin, "Design of low-density parity-check codes for modulation and detection," *IEEE Trans. Commun.*, vol. 52, no. 4, pp. 670–678, Apr. 2004.
- [31] I. Andriyanova and E. Soljanin, "Optimized IR-HARQ schemes based on punctured LDPC codes over the BEC," *IEEE Trans. Inf. Theory*, vol. 58, no. 10, pp. 6433–6445, Oct. 2012.
- [32] R. Xu, P. Chen, M. Zhu, and B. Bai, "A reliability-based adaptive IR-HARQ scheme for polar coded systems," in *Proc. Int. Conf. Wireless Commun. Signal Process. (WCSP)*, Oct. 2020, pp. 871–876.



**Xiaoxi Yu** received the B.Eng. degree in electrical and electronics engineering and the M.S. degree in wireless communications and signal processing from the University of Bristol in September 2016 and February 2018, respectively. She is currently pursuing the Ph.D. degree with Nanyang Technological University, Singapore. Her research interests include information and coding theory, LDPC/protograph codes, and HARQ schemes.



**Md. Noor-A-Rahim** received the Ph.D. degree from the Institute for Telecommunications Research, University of South Australia, Adelaide, Australia, in 2015. He is currently a Lecturer (Assistant Professor) with the School of Computer Science and Information Technology, University College Cork, Ireland. Prior to this role, he was a Marie Curie Fellow with the School of Computer Science and Information Technology, University College Cork. He also held the position of a Post-Doctoral Research Fellow with the Centre for Infocomm Technology (INFINTUS), Nanyang Technological University (NTU), Singapore. His research interests include intelligent transportation systems, machine learning, the Internet of Things, and signal processing. In recognition of his academic excellence, he was honored with the Michael Miller Medal from the Institute for Telecommunications Research (ITR), University of South Australia, for presenting the most outstanding Ph.D. thesis in 2015.



**Yong Liang Guan** (Senior Member, IEEE) received the Bachelor of Engineering degree (Hons.) from the National University of Singapore and the Ph.D. degree from Imperial College London, U.K. He is currently a Professor of communication engineering with the School of Electrical and Electronic Engineering, Nanyang Technological University (NTU), Singapore, where he leads the Continental-NTU Corporate Research Laboratory and led the successful deployment of the campus-wide NTU-NXP V2X test bed. He is also an Associate Vice President of

NTU. He has secured over \$70 million of external research funding. He has published an invited monograph, two books, and more than 450 journal articles and conference papers. He has 15 filed patents and three granted patents, one of which was licensed to NXP Semiconductors. His research interests include coding and signal processing for communication systems and data storage systems. He is an Editor of the *IEEE TRANSACTIONS ON VEHICULAR TECHNOLOGY*. He is also a Distinguished Lecturer of the IEEE Vehicular Technology Society.



**Zhaojie Yang** received the B.Sc. degree in electronic engineering from Lingnan Normal University, China, in 2016, and the Ph.D. degree in communication engineering from the Guangdong University of Technology, China, in 2021. From November 2020 to October 2021, he was a Visiting Student with the Department of Electronic and Information Engineering, The Hong Kong Polytechnic University, Hong Kong. He is currently a Research Fellow with the School of Electrical and Electronic Engineering, Nanyang Technological University, Singapore. His research interests include channel coding, high-order modulations, and spatial modulations.



**Li Deng** received the Ph.D. degree from the National Key Laboratory of Wireless Communications, University of Electronic Science and Technology of China, in 2021. From 2019 to 2020, she spent one year as a Visiting Scholar with the School of Electrical and Electronic Engineering, Nanyang Technological University, Singapore. She is currently a Post-Doctoral Research Fellow with the University of Electronic Science and Technology of China. She is also a Professor with the School of Electronic Information and Automation, Guilin University of Aerospace Technology. Her research interests include information and coding theory and image communication.

and coding theory and image communication.



**Zhiping Shi** received the master's and Ph.D. degrees from Southwest Jiaotong University, Chengdu, China, in 1998 and 2005, respectively. She has two years of post-doctoral experience with the University of Electronic Science and Technology of China (UESTC) from 2005 to 2007. In 2007, she joined the School of Communication and Information, UESTC. From 2009 to 2010, she spent one year as a Visiting Scholar with Lehigh University, Bethlehem, PA, USA. She is currently a Professor with the National Key Laboratory of Communications, UESTC. Her

research interests include coding theory, cognitive radio, and wireless communications.